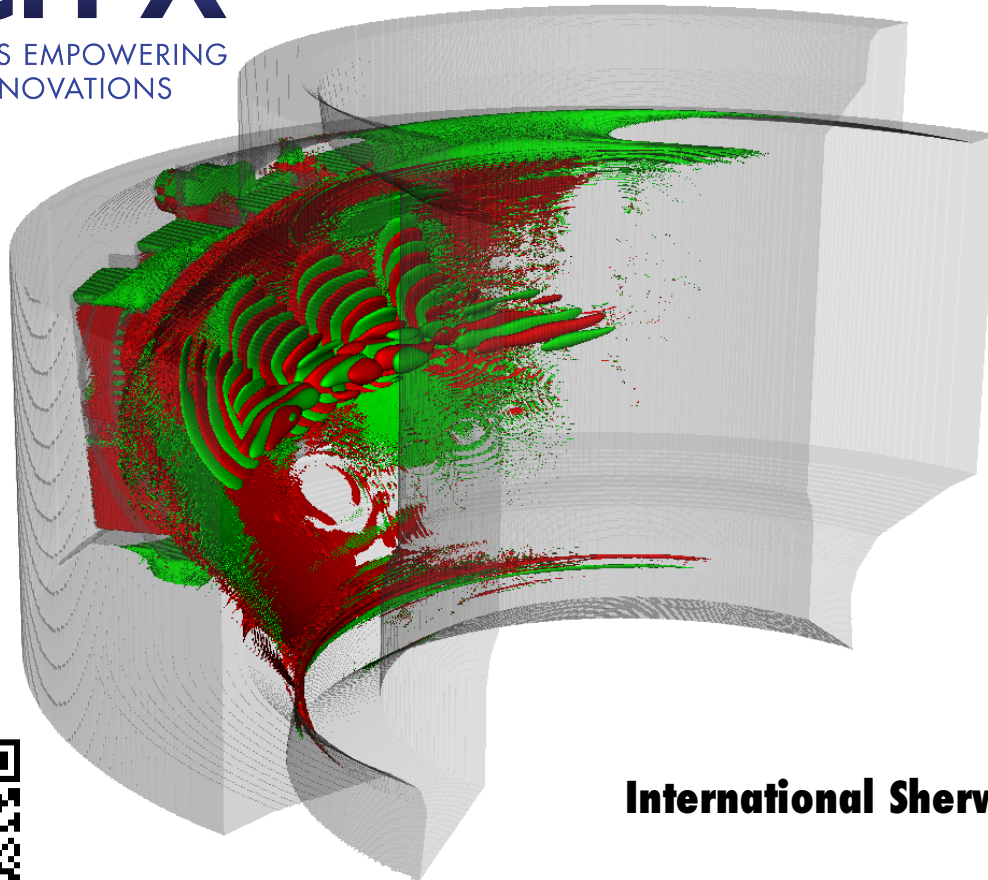




VORPAL MODELING OF FUSION-RELEVANT RF PROCESSES IN THE SCRAPE-OFF LAYER

TECH-X

SIMULATIONS EMPOWERING
YOUR INNOVATIONS



Thomas G. Jenkins
David N. Smithe

Tech-X Corporation

**(with other members of the SciDAC
Center for Integrated Simulation
of Fusion-Relevant RF Actuators,
and associated collaborators)**



www.txcorp.com

International Sherwood Fusion Theory Conference
Auburn, AL
April 23, 2018



Abstract

The development of robust radiofrequency (RF) actuators for plasma heating and current drive will be critical in sustaining steady-state operation of future magnetic fusion devices. As part of this development, an increased understanding of how applied RF power interacts with the scrape-off layer (SOL) plasma, as well as with plasma sheaths formed near material surfaces such as antenna hardware, is sought.

We summarize a number of ongoing efforts to numerically model these interactions using Vorpal, a high-performance particle-in-cell/finite-difference time-domain code; eventual couplings of Vorpal with materials, turbulence, and transport codes are anticipated as part of ongoing work by the RF-SciDAC group. Present efforts include (a) particle-in-cell (PIC) modeling of sheath rectification in time-varying RF sheaths on antenna surfaces, and the benchmarking of these results against other RF-SciDAC codes; (b) comparison of experimentally measured electric fields in the RF sheath with Vorpal models; (c) computation of ponderomotive force terms near the antenna hardware, which arise as RF power passes through the SOL; and (d) modeling of RF scattering from SOL turbulence. Ongoing progress in these areas will be discussed.

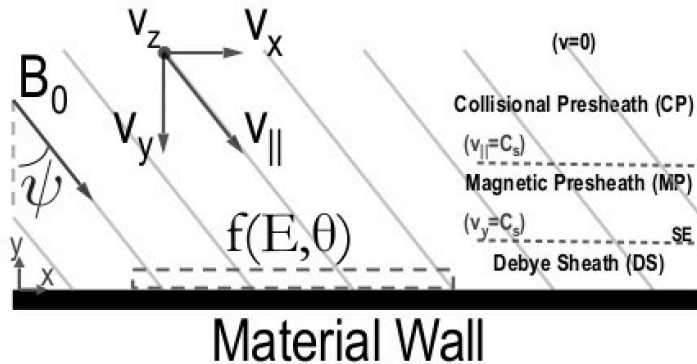
Supported by the SciDAC Center for Integrated Simulation of Fusion-Relevant RF Actuators (DE-SC0018319).



Plasma sheath formation on RF antenna surfaces: a multiscale problem

- Sheath formation on antenna surfaces is associated with sputtering of neutral wall atoms, and subsequent high-Z impurity contamination of the fusion reaction as these neutrals are ionized.
- Sheath widths are small relative to characteristic RF wavelengths, but still drive relevant physics. Problem is highly multiscale:
 $\{\lambda_{RF}, \Delta_{sheath}, \lambda_{mfp}, L_{device}\}$ and $\{\omega_{pe}, \omega_{RF}, \Omega_i, \nu_{coll}\}$
- Both the ion distribution function in the sheath and the sheath structure itself are affected by magnetic fields and RF bias.
- Working with materials scientists at UIUC to benchmark RF and PMI codes, as starting point. Use 1D3V simulation with constant B-field to begin with: see R. Khaziev and D. Curreli, Phys. Plasmas **22**, 043503 (2015).
- **hPIC** – full-f electrostatic PIC code, kinetic ions, kinetic (Boris-Buneman) or adiabatic electrons, scales to tens of thousands of cores
- **Vorpal** (VSim) – electromagnetic/electrostatic PIC code, kinetic (Boris) particles, scales to hundreds of thousands of cores

RF-SciDAC code benchmarking activities



$$\psi = 70^\circ, T = 3 \text{ eV}, \quad \vec{B} = 1 \text{ T},$$

$$n = 5.0 \times \frac{10^{16}}{\text{m}^3}, \quad \frac{m_e}{m_i} = 1836$$

$$PPC = 500, \quad \Delta x = \frac{\lambda_{De}}{2}, \quad \Delta t = \frac{2\pi}{20 \cdot \Omega_e}$$

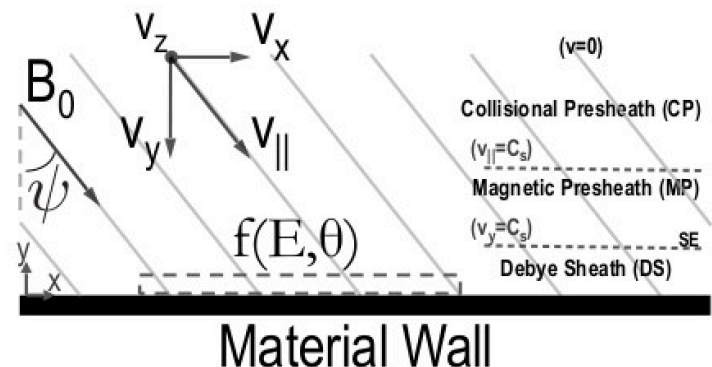
Lost particles replenished with volumetric source

- Multiple benchmark cases specified, to verify code consistency:
 - case 0: unmagnetized, grounded walls
 - case 1: magnetized, grounded walls
 - case 2: magnetized, grounded left wall, right wall at $V = 10T_e/q$ volts
 - case 3: magnetized, grounded left wall, right wall at $V = V_0 \sin(\omega t)$, with RF frequency ω taking various values in relation to ω_{pi}
- Compare n , Γ , drift velocities, heat flux, ϕ , electric field in each case
- Thereafter, will add specified impurity fluxes from wall (fixed source, or self-consistent with PMI models).
- Will also compare initial cases with other RF-SciDAC codes (RF-SOL, Petra-M, BOUT++) and models (Myra generalized sheath BC) where possible

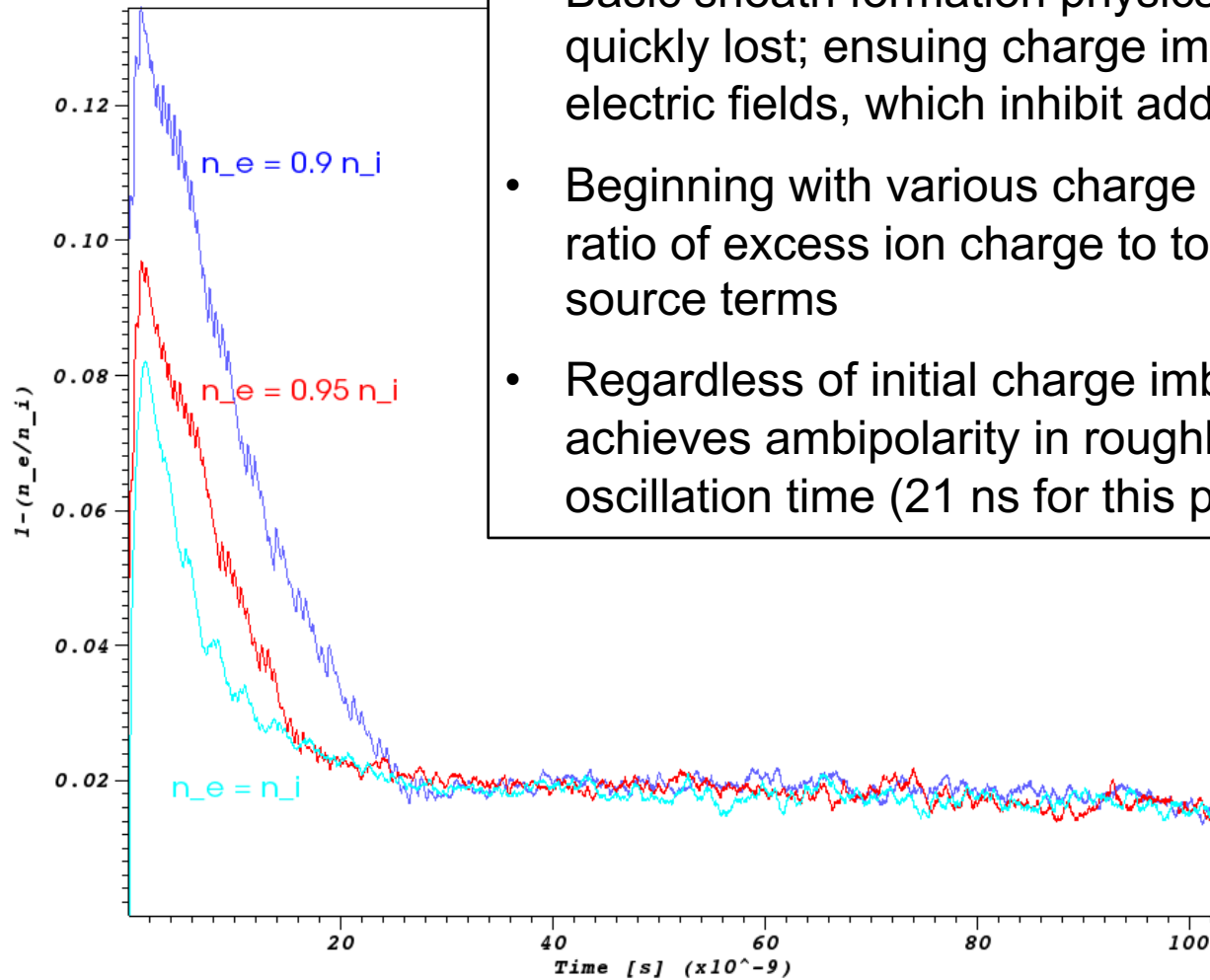
Analytical expressions for particle velocities can be determined for simple cases

$$\begin{aligned}
 v_x(t) &= v_{x0}[\sin^2 \psi + \cos^2 \psi \cos(\Omega_\alpha t)] + v_{y0} \cos \psi \sin(\Omega_\alpha t) + v_{z0} \sin \psi \cos \psi [1 - \cos(\Omega_\alpha t)] \\
 &\quad + \frac{q_\alpha}{m_\alpha} \sin^2 \psi \int_0^t E_x(x, t') dt' + \frac{q_\alpha}{m_\alpha} \cos^2 \psi \int_0^t E_x(x, t') \cos[\Omega_\alpha(t - t')] dt' \\
 v_y(t) &= v_{x0} \cos \psi \sin(\Omega_\alpha t) + v_{y0} \cos(\Omega_\alpha t) + v_{z0} \sin \psi \sin(\Omega_\alpha t) - \frac{q_\alpha}{m_\alpha} \cos \psi \int_0^t E_x(x, t') \sin[\Omega_\alpha(t - t')] dt' \\
 v_z(t) &= v_{x0} \sin \psi \cos \psi [1 - \cos(\Omega_\alpha t)] - v_{y0} \sin \psi \sin(\Omega_\alpha t) + v_{z0} [\cos^2 \psi + \sin^2 \psi \cos(\Omega_\alpha t)] \\
 &\quad + \frac{q_\alpha}{m_\alpha} \sin \psi \cos \psi \int_0^t E_x(x, t') dt' - \frac{q_\alpha}{m_\alpha} \sin \psi \cos \psi \int_0^t E_x(x, t') \cos[\Omega_\alpha(t - t')] dt'
 \end{aligned}$$

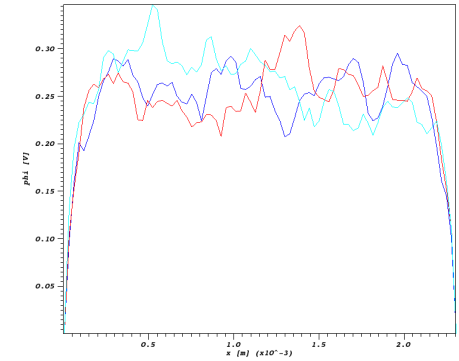
For 1D3D simulations, provides useful code verification metric.



Sheath physics is somewhat insensitive to plasma sources



- Basic sheath formation physics – electrons are quickly lost; ensuing charge imbalance creates electric fields, which inhibit additional electron loss
- Beginning with various charge imbalances, look at ratio of excess ion charge to total ion charge, no source terms
- Regardless of initial charge imbalance, plasma achieves ambipolarity in roughly an ion plasma oscillation time (21 ns for this plasma)



Comparison of experimentally measured sheath electric fields with simulation

- Elijah Martin (ORNL) has developed non-intrusive diagnostic techniques to measure sheath electric fields with spectroscopy (see Martin *et al.*, PPCF **57**(6), 065011 (2015) and Klepper *et al.*, PRL **110**(21), 215005 (2013)).
- Data from SERF (Sheath Experiment for RF) experiment at ORNL to be compared with simulations from Vorpal, other RF-SciDAC codes

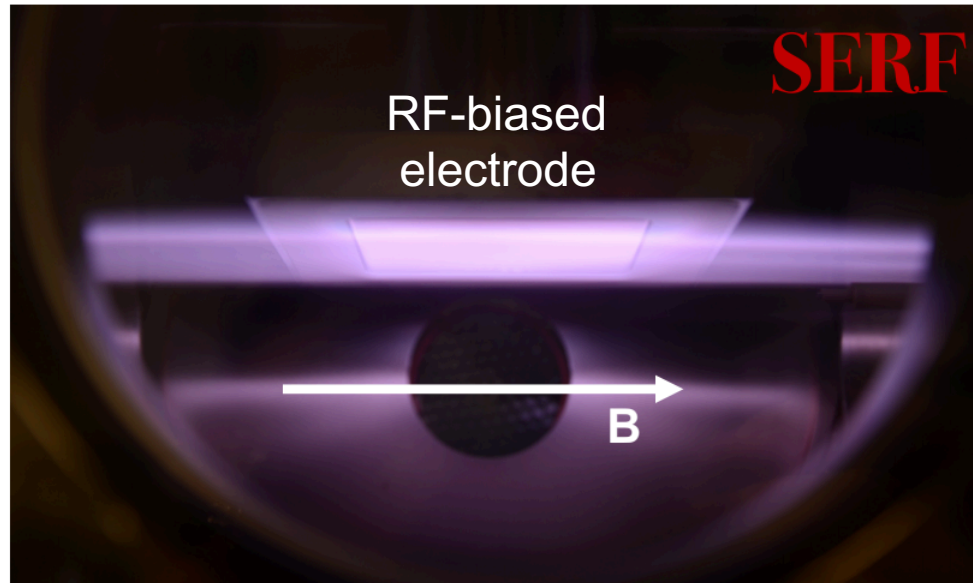
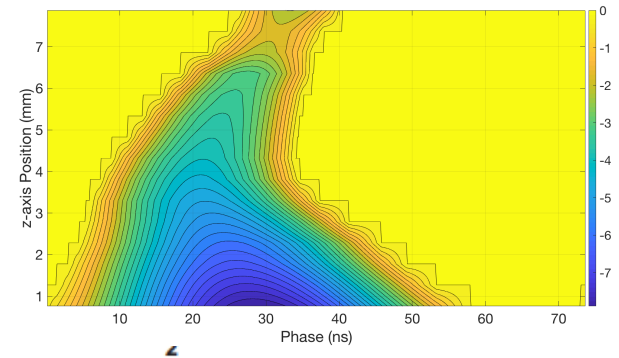
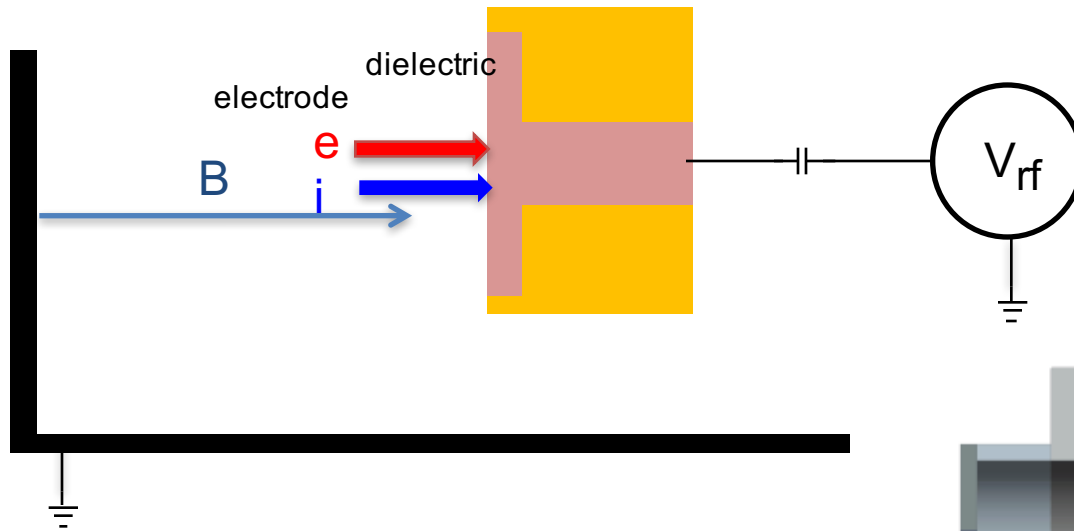


Figure courtesy E. Martin

ORNL experiment can be run in parallel or perpendicular configurations

ORNL RF test stand with floating electrode having E_{RF} parallel to B

- Electrons and ions are not confined in sheath. Should follow the non-magnetized sheath theory.
- Floating electrode develops a negative DC bias with respect to plasma to repel most electrons
- Non-neutral sheath surrounds electrode: face



Line of sight for E_{RF} parallel to B is into the page. The spatial coordinate is with respect to electrode surface normal.

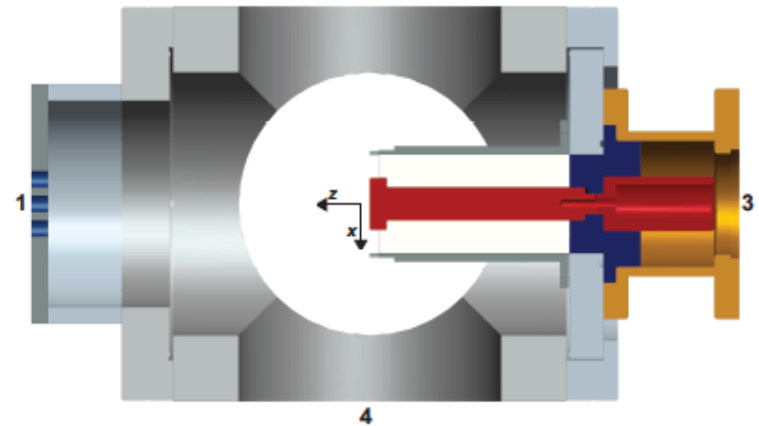
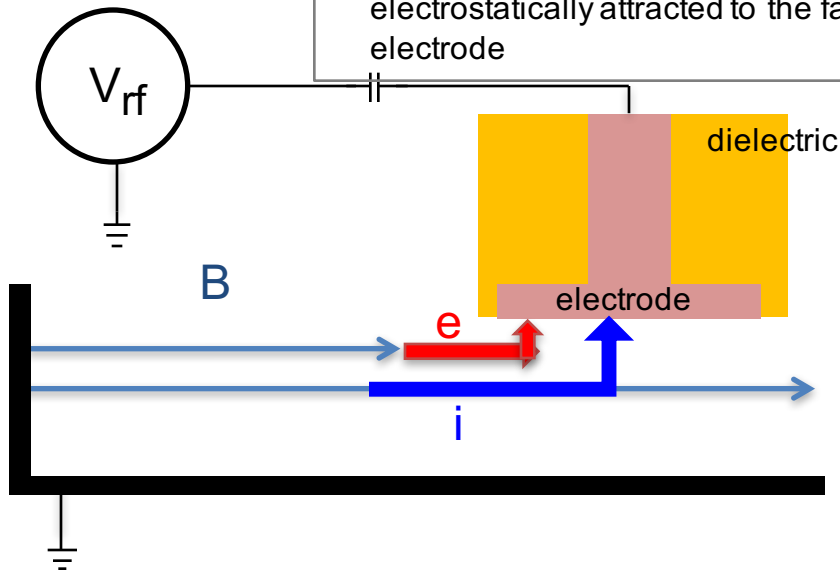


Figure 4.1: Experimental setup for the parallel field configuration.

ORNL experiment can be run in parallel or perpendicular configurations

ORNL RF test stand with floating electrode having E_{RF} perpendicular to B

- Electrons are collected within a few gyroradii at the electrode surface (gyroradii are on the order of 1 to 2 mm because electron has accelerated to ~ 3 keV)
- Floating electrode develops a negative DC bias with respect to plasma, to repel most electrons
- Non-neutral sheath surrounds electrode: edge and face
- Weakly magnetized ($\Omega_i \ll \omega_{pi}$) ions are electrostatically attracted to the face of the electrode



Line of sight for E_{RF} perpendicular to B is into the page. The spatial coordinate is with respect to electrode surface normal.

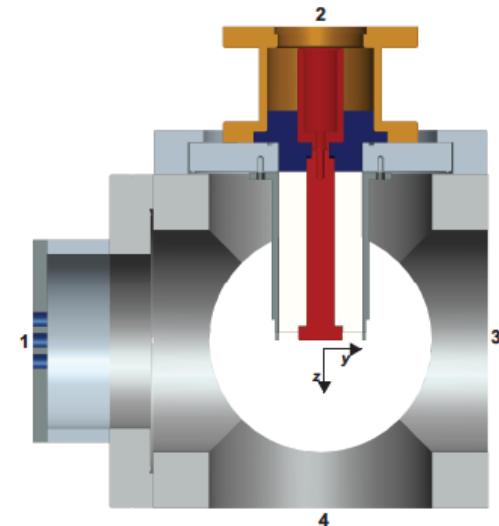
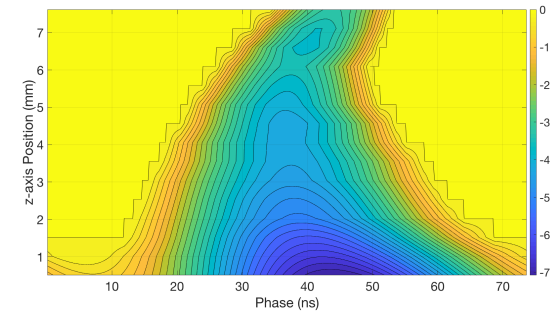


Figure 4.2: Experimental setup for the perpendicular field configuration.

Ponderomotive forces and RF

- Single-species fluid momentum equation – use current, not velocity, form:

$$m_\alpha n_\alpha \frac{\partial \vec{V}_\alpha}{\partial t} + m_\alpha n_\alpha (\vec{V}_\alpha \cdot \vec{\nabla}) \vec{V}_\alpha + \vec{\nabla} \cdot \vec{P}_\alpha = \rho_\alpha [\vec{E} + \vec{V}_\alpha \times \vec{B}] + \text{collisions} + \text{sources}$$

$$\frac{m_\alpha}{q_\alpha} \frac{\partial \vec{J}_\alpha}{\partial t} + \frac{m_\alpha}{q_\alpha} \vec{\nabla} \cdot \left(\frac{\vec{J}_\alpha \vec{J}_\alpha}{\rho_\alpha} \right) + \vec{\nabla} \cdot \vec{P}_\alpha = [\rho_\alpha \vec{E} + \vec{J}_\alpha \times \vec{B}] + \text{collisions} + \text{sources}$$

- Has both slow and fast timescale quantities; products of fast-timescale perturbations can beat down into slow-timescale dynamics.
- Not linearization – spectral decomposition. (Maxwell equations separable.)

$$\frac{(\vec{J}_{\alpha 0} + \vec{J}_{\alpha 1})(\vec{J}_{\alpha 0} + \vec{J}_{\alpha 1})}{(\rho_{\alpha 0} + \rho_{\alpha 1})} = \frac{\vec{J}_{\alpha 0} \vec{J}_{\alpha 0}}{\rho_{\alpha 0}} + \frac{\vec{J}_{\alpha 0} \vec{J}_{\alpha 1}}{\rho_{\alpha 0}} + \frac{\vec{J}_{\alpha 1} \vec{J}_{\alpha 0}}{\rho_{\alpha 0}} - \frac{\rho_{\alpha 1} \vec{J}_{\alpha 0} \vec{J}_{\alpha 0}}{\rho_{\alpha 0}^2}$$

$$+ \frac{\left(\vec{J}_{\alpha 1} - \frac{\rho_{\alpha 1} \vec{J}_{\alpha 0}}{\rho_{\alpha 0}} \right) \left(\vec{J}_{\alpha 1} - \frac{\rho_{\alpha 1} \vec{J}_{\alpha 0}}{\rho_{\alpha 0}} \right)}{(\rho_{\alpha 0} + \rho_{\alpha 1})} \quad \begin{array}{l} = \text{slow} + \text{fast} \\ + \text{quasilinear} \end{array}$$

$$\rho_\alpha \vec{E} + \vec{J}_\alpha \times \vec{B} = \rho_{\alpha 0} \vec{E}_0 + \vec{J}_{\alpha 0} \times \vec{B}_0 + \rho_{\alpha 1} \vec{E}_0 + \vec{J}_{\alpha 1} \times \vec{B}_0 + \rho_{\alpha 0} \vec{E}_1 + \vec{J}_{\alpha 0} \times \vec{B}_1 + \rho_{\alpha 1} \vec{E}_1 + \vec{J}_{\alpha 1} \times \vec{B}_1$$

Applying high-pass and low-pass filters yields separable equations for fast/slow timescales

Slow:

$$\left\langle \frac{m_\alpha}{q_\alpha} \frac{\partial \vec{J}_{\alpha 0}}{\partial t} \right\rangle_{LP} + \left\langle \frac{m_\alpha}{q_\alpha} \vec{\nabla} \cdot \left(\frac{\vec{J}_{\alpha 0} \vec{J}_{\alpha 0}}{\rho_{\alpha 0}} \right) \right\rangle_{LP} + \langle \vec{\nabla} \cdot \vec{P}_{\alpha 0} \rangle_{LP}$$

$$+ \left\langle \frac{m_\alpha}{q_\alpha} \vec{\nabla} \cdot \left[\frac{\left(\vec{J}_{\alpha 1} - \frac{\rho_{\alpha 1} \vec{J}_{\alpha 0}}{\rho_{\alpha 0}} \right) \left(\vec{J}_{\alpha 1} - \frac{\rho_{\alpha 1} \vec{J}_{\alpha 0}}{\rho_{\alpha 0}} \right)}{(\rho_{\alpha 0} + \rho_{\alpha 1})} \right] \right\rangle_{LP} - \langle [\rho_{\alpha 1} \vec{E}_1 + \vec{J}_{\alpha 1} \times \vec{B}_1] \rangle_{LP}$$

$$= \langle [\rho_{\alpha 0} \vec{E}_0 + \vec{J}_{\alpha 0} \times \vec{B}_0] \rangle_{LP} + \langle \text{collisions} \rangle_{LP} + \langle \text{sources} \rangle_{LP}$$

Fast:

$$\left\langle \frac{m_\alpha}{q_\alpha} \frac{\partial \vec{J}_{\alpha 1}}{\partial t} \right\rangle_{HP} + \left\langle \frac{m_\alpha}{q_\alpha} \vec{\nabla} \cdot \left(\frac{\vec{J}_{\alpha 0} \vec{J}_{\alpha 1}}{\rho_{\alpha 0}} + \frac{\vec{J}_{\alpha 1} \vec{J}_{\alpha 0}}{\rho_{\alpha 0}} - \frac{\rho_{\alpha 1} \vec{J}_{\alpha 0} \vec{J}_{\alpha 0}}{\rho_{\alpha 0}^2} \right) \right\rangle_{HP} + \langle \vec{\nabla} \cdot \vec{P}_{\alpha 1} \rangle_{HP}$$

$$+ \left\langle \frac{m_\alpha}{q_\alpha} \vec{\nabla} \cdot \left[\frac{\left(\vec{J}_{\alpha 1} - \frac{\rho_{\alpha 1} \vec{J}_{\alpha 0}}{\rho_{\alpha 0}} \right) \left(\vec{J}_{\alpha 1} - \frac{\rho_{\alpha 1} \vec{J}_{\alpha 0}}{\rho_{\alpha 0}} \right)}{(\rho_{\alpha 0} + \rho_{\alpha 1})} \right] \right\rangle_{HP}$$

$$= \langle [\rho_{\alpha 1} \vec{E}_0 + \vec{J}_{\alpha 1} \times \vec{B}_0 + \rho_{\alpha 0} \vec{E}_1 + \vec{J}_{\alpha 0} \times \vec{B}_1] \rangle_{HP} + \langle \text{collisions} \rangle_{HP} + \langle \text{sources} \rangle_{HP}$$

Fast-timescale equation – limiting behavior

- Ignoring finite temperature effects, zeroth-order flows and electric fields, collisions, and sources, the fast timescale equation reduces to

$$\left\langle \frac{m_\alpha}{q_\alpha} \frac{\partial \vec{J}_{\alpha 1}}{\partial t} \right\rangle_{HP} = \langle [\vec{J}_{\alpha 1} \times \vec{B}_0 + \rho_{\alpha 0} \vec{E}_1] \rangle_{HP}$$

(the standard cold magnetized plasma current equation). Vorpahl already solves this equation.

Slow-timescale equation – bulk behavior

- Summing over species allows the slow timescale equation to be written with a generalized pressure tensor,

$$\begin{aligned}
 & \left\langle \frac{\partial}{\partial t} \left[\Sigma_{\alpha} \frac{m_{\alpha} \vec{J}_{\alpha 0}}{q_{\alpha}} + \epsilon_0 (\vec{E}_1 \times \vec{B}_1) \right] \right\rangle_{LP} + \vec{\nabla} \cdot \left\langle \vec{P}_{\alpha 0} + \Sigma_{\alpha} \frac{m_{\alpha} \vec{J}_{\alpha 0} \vec{J}_{\alpha 0}}{q_{\alpha} \rho_{\alpha 0}} \right\rangle_{LP} \\
 & + \vec{\nabla} \cdot \left\langle \frac{\epsilon_0 |\vec{E}_1|^2 \vec{I}}{2} - \epsilon_0 \vec{E}_1 \vec{E}_1 + \frac{|\vec{B}_1|^2 \vec{I}}{2\mu_0} - \frac{\vec{B}_1 \vec{B}_1}{\mu_0} + \Sigma_{\alpha} \frac{m_{\alpha}}{q_{\alpha}} \left[\frac{\left(\vec{J}_{\alpha 1} - \frac{\rho_{\alpha 1} \vec{J}_{\alpha 0}}{\rho_{\alpha 0}} \right) \left(\vec{J}_{\alpha 1} - \frac{\rho_{\alpha 1} \vec{J}_{\alpha 0}}{\rho_{\alpha 0}} \right)}{(\rho_{\alpha 0} + \rho_{\alpha 1})} \right] \right\rangle_{LP} \\
 & = \langle [\rho_0 \vec{E}_0 + \vec{J}_0 \times \vec{B}_0] \rangle_{LP} + \langle \text{collisions} \rangle_{LP} + \langle \text{sources} \rangle_{LP}
 \end{aligned}$$

For edge/SOL plasma, many terms can be comparable – cannot drop any terms.



Summary of upcoming RF-SciDAC work at Tech-X

- Benchmarking of Vorpil sheath modeling with other RF-SciDAC codes and models
- Comparison of Vorpil sheath modeling with SERF experiment
- Vorpil modeling of ponderomotive forces during ICRF antenna operation